CHEMICAL ENGINEERING TRANSACTIONS
VOL. 55, 2016
A publication of AIDIC
The Italian Association of Chemical Engineering
Online at www.aidic.it/cet
Guest Editors:Tichun Wang, Hongyang Zhang, Lei Tian

ISBN978-88-95608-46-4; **ISSN** 2283-9216
DOI: 10.3303/CET1655044

Preparation, Characterization and Properties of SiO_2 Aerogel Composite Thermal Insulation Coating

Zhaohui Liu, Yidong Ding*, Xin Shu, Na Liu

Department of Chemistry & Materials Engineering, LEU, Chongqing, China
419659327@qq.com

Probing into the preparation and thermal insulation mechanism of SiO_2 aerogel composite thermal insulation coating, it is discovered that the thermal insulation and heat control of the coating are realized by means of reducing the thermal conductivity, increasing the reflectivity and radiance, etc. The author obtains the content of each filler by single-doped experiments, acquires the optimal coating formula by orthogonal experiment, and gets the characteristics of the coating with self-made thermal insulation test equipment, scanning electron microscope (SEM), fourier translation infrared spectrum (FT-IR), X-ray diffractometer (XRD) and other analytical methods. The results show that the SiO_2 aerogel composite thermal insulation coating has the best performance when 5ωt% SiO_2 aerogel, 5ωt% titanium dioxide, 5ωt% hollow glass beads, and 10ωt% far-infrared ceramic powder are added. Besides, the high temperature performance of the coating improves with the increase of mass fraction of SiO_2 aerogel. When the fraction is 5ωt%, the SiO_2 aerogel composite thermal insulation coating performs well at 300°C. Therefore, the author concludes that the SiO_2 aerogel significantly improves the thermal insulation and high temperature performance of the thermal insulation coating. The conclusion lays a good foundation for the application of SiO_2 aerogel in the coating industry.

1. Introduction

The rapid socio-economic development has spurred an increase in energy consumption and raised the awareness of building energy efficiency. Fortunately, there are many innovations in the field of building energy conservation that have significantly improved energy efficiency. The R&D and application of new thermal insulation materials are not to be ignored (Lang, 2002). As one of the ten most promising new materials, SiO_2 aerogel boasts broad prospects in building thermal insulation (Buratti et al., 2016l Cheng and Cheng, 2012). Thanks to its unique nano-pore and 3D network structure, the material can effectively reduce the heat transfer, thereby protecting the environment and reducing energy consumption (Boulaoued et al., 2016; De Angelis et al., 2016; Luca et al., 2016; Mario et al., 2013; Zhou and chen, 2016; Woignier et al., 1990; Pierre and Pajonk, 2002; Roselli et al., 2016). Insulation coating refers to the functional coating with thermal insulation effect. By the mechanism of action, insulation coating is mainly divided into reflective insulation coating, thermal barrier coating, and radiant insulation coating. Due to the stricter requirements on insulation performance nowadays, the R&D of composite thermal insulation coating material has become a new hotspot (Xia et al., 2001; Lu and Chen, 2005). The so-called composite thermal insulation coating material stands for the thermal insulation coating material of two or more insulation mechanisms. Different thermal insulation materials are combined into one so that several insulation mechanisms can act at the same time. With the synergic effect of various insulation measures, the composite coating material has a better effect than coating materials of only one insulation mechanism. However, the multiple thermal insulation effect of the composite coating material depends on the low thermal conductivity, high reflectivity and radiance of the functional fillers. Normally, two or more fillers should be mixed together. If SiO_2 aerogel is applied, the thermal conductivity of the insulation coating would decrease dramatically, thereby improving the insulation effect (Qu et al., 2014; Zhao et al., 2014). This paper optimizes the formula of the coating by using SiO_2 aerogel as the barrier filler, titanium dioxide and hollow glass beads as the reflective filler, and far-infrared ceramic powder as reflective powder. In this way, the author obtains SiO_2 aerogel composite thermal insulation coating with excellent thermal insulation performance, and explores its high temperature performance.

Please cite this article as: Liu Z.H., Ding Y.D., Shu X., Liu N., 2016, Preparation, characterization and properties of sio2 aerogel composite thermal insulation coating, Chemical Engineering Transactions, 55, 259-264 DOI:10.3303/CET1655044

2. Test

2.1 Raw materials

Hydrophobic SiO_2 aerogel (Guangdong Alison Hi-Tech Co. ,Ltd.); silicone-based wetting agent Silok 7117, Alkyl ammonium salt dispersant Silok 7195 (Silok); water-based acrylic resin, film-forming additives (Jelee Chemical Industry); titanium dioxide (Huntsman); hollow glass beads (3M); far-infrared ceramic powder (Lingshou County Xunhang Mineral Distribution Co., Ltd.); defoamer 681-F (Rhodia); deionized water (lab made).

2.2 Coating preparation

The SiO_2 aerogel composite thermal insulation coating material is prepared in the following process: Firstly, mix the SiO_2 aerogel particles with multi-grade zirconium beads, grind the particles into nano powder with a high-energy ball mill (speed: 500r/min; duration: 5min; cycle: 1). Secondly, add wetting agent, dispersant, deionized water and a certain amount of zirconium beads into a beaker and stir the mixture evenly (speed: 300~500r/min; duration: 3 minutes). Thirdly, add some defoamer dropwise into the beaker, add the SiO_2 aerogel powder, and let the mixture disperse for 3h (speed: 1,800r/min); To prevent the powder from flying at the beginning, the beaker cup should be sealed. Meanwhile, reduce the speed to 700r/min to remove the bubbles in the coating material. While adding the rest of the defoamer, prepare evenly dispersed and stable SiO_2 aerogel slurry by slowing down the speed in stages. Fourthly, mix the SiO_2 aerogel slurry with resin and additives, add titanium dioxide, far-infrared ceramic powder and hollow glass beads in turn, mix and stir the materials to get the coating material. After the addition of titanium dioxide and far-infrared ceramic powder, high-speed shear dispersion can be adopted (speed: 1,000r/min; duration: 20m); Before the addition of hollow glass beads, the speed should be reduced to 500r/min to prevent excessive shear force from breaking the outer wall of hollow glass beads, causing damages to the hollow insulation structure of the hollow glass beads.

2.3 Performance test

The test is performed in accordance with the *Roofing Products from Metal Sheet with Reflect Thermal Coating*. In light of actual needs, the author improves the standard test device by making a thermal insulation test device with polystyrene foam (thickness: 30mm; thermal conductivity: 0.025 W/(m•K)) for the sample coating. The coating is characterized with scanning electron microscope (SEM), fourier translation infrared spectrum (FT-IR), and X-ray diffractometer (XRD). With different sized wire rod coaters, the author prepares coatings of different film thicknesses, and characterizes their insulation performance. In addition, the author heats the coatings to 200°C, 300°C and 400°C in a muffle furnace, and analyzes their high temperature performances with XRD and FT-IR.

3. Results and discussion

3.1 Thermal insulation performance of SiO_2 aerogel composite thermal insulation coating

3.1.1 Formula optimization of SiO_2 aerogel composite thermal insulation coating

By the mechanism of action, insulation coating is mainly divided into reflective insulation coating, thermal barrier coating, and radiant insulation coating. In the test, the insulation coating is prepared with functional fillers like SiO_2 aerogel, titanium dioxide, hollow glass beads, and far-infrared ceramic powder. When the insulation coating is made of a single kind of filler, it has the best performance when 5ωt% SiO_2 aerogel, 5ωt% titanium dioxide, 5ωt% hollow glass beads, and 8ωt% far-infrared ceramic powder are added respectively. In the experiment, the functional fillers are added in combinations so that the coating features low thermal conductivity, high reflectivity and high radiance. Besides, the author optimizes the formula of SiO_2 aerogel composite thermal insulation coating based on the equilibrium temperature of the bottom of the sample coating in the orthogonal test. Table 1 records the data of the test, where the ωt% of titanium dioxide and hollow glass beads are obtained after the two fillers are mixed at the ratio of 1:1.

According to Table 1, the values in the column of SiO_2 aerogel are greater than those in other columns within the range R, indicating that the SiO_2 aerogel consumption of the coating formula has the most significant impact on the thermal insulation performance of the optimized SiO_2 aerogel thermal insulation coating, followed by the consumption of titanium dioxide and the consumption of hollow glass beads. The far-infrared ceramic powder has the lowest impact to the thermal insulation performance of the coating. The optimal ratio between the fillers is SiO_2 aerogel: titanium dioxide: hollow glass beads: far-infrared ceramic powder= 5: 5: 5: 10. At this ratio, the bottom temperature of the sample coating is 44.4°C, 14.8°C lower than the equilibrium temperature at the bottom of the uncoated blank sample. This means the ratio has a good insulation effect.

Table 1: Orthogonal test of $L_9(3^4)$

Number	Content (ωt%)			
	SiO_2 aerogel	TiO_2 and Hollow glass beads	Far-infrared ceramic powder	Temperature (°C)
1	4	8	6	47.2
2	4	10	8	46
3	4	12	10	46.6
4	5	8	8	45.5
5	5	10	10	44.4
6	5	12	6	45
7	6	8	10	48.2
8	6	10	6	47.8
9	6	12	8	49.5
K_1	139.8	140.9	140	
K_2	134.9	138.2	141	
K_3	145.5	141.1	139.2	
k_1	46.6	46.9667	46.6667	
k_2	44.9667	46.0667	47	
k_3	48.5	47.0333	46.4	
Range R	3.5333	0.9666	0.6	

3.1.2 The effect of film thickness on thermal insulation performance

According to the test results in Section 2.1.1, the author prepares coatings at the thickness of 50μm, 80μm, 100μm, 150μm and 200μm with a coater and in light of the optimal formula of five materials. In other words, the author adopts the optimal ratio between the fillers SiO_2 aerogel: titanium dioxide: hollow glass beads: far-infrared ceramic powder= 5: 5: 5: 10. After the coatings are solidified at room temperature, the author measures the equilibrium temperatures of the sample coatings. See Figure 1 for the test results.

As shown in Figure 1, the equilibrium temperatures of the sample coatings gradually decrease with the increase of the coating thickness, but the downward trend gradually slows. The phenomenon is interpreted as follows: the thicker the coating, the more functional fillers in a unit area, leading to a decrease in thermal conductivity, and an increase in reflectivity and radiance. As a result, the thermal insulation performance of the coating gets better as the thickness grows. When the wet film thickness is 100μm, 150μm and 200μm, the equilibrium temperature of the sample coating is 44.6°C, 44.2°C and 44°C respectively. This indicates that the thermal insulation performance of the coating is not significantly improved after the thickness exceeds a certain degree due to the lack of sufficient decrease of thermal conductivity or increase of solar reflectance and radiance.

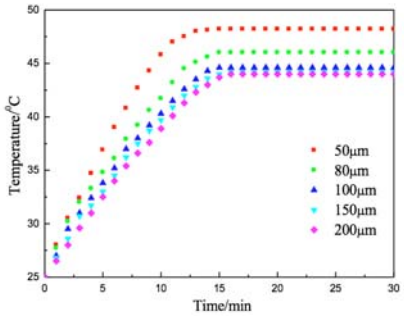

Figure 1: The change curve of temperatures of sample coatings of different thicknesses

3.2 Analysis and characterization of SiO_2 aerogel composite thermal insulation coating

3.2.1 Micro-morphology analysis

Figure 2 displays the SEM images of the SiO_2 aerogel composite thermal insulation coatings of formula 5 and formula 6, which have better thermal insulation performance than the coatings of other formulas. As shown in the figure, the hollow glass beads form a continuous solar barrier layer and reflective layer, featuring low

thermal conductivity and reflection effect. Due to their small particle sizes, SiO_2 aerogel, titanium dioxide and far-infrared ceramic powder fill up the gaps of the coating, which enhances the continuity of filler and improves the barrier efficiency of the coating; some of these materials are attached to the surface of the hollow glass beads, acting as a reflector and radiator of sunlight (Garbarino et al., 2013; Liang, 2014; Feng et al., 2017).

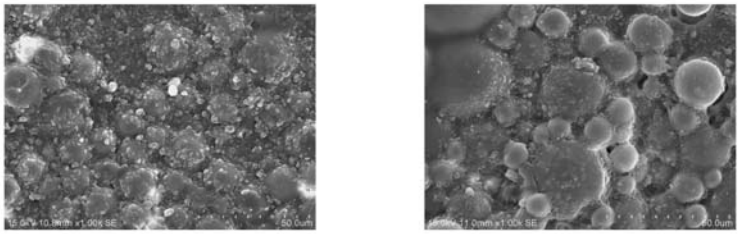

(a) Coating of formulation 5 (b) Coating of formulation6

Figure 2: SEM images of SiO_2 aerogel composite thermal insulation coatings of different formulas

3.2.2 FT-IR analysis

Figure 3 displays the infrared images of SiO_2 aerogel composite insulation coatings of different formulas. As show in the figure, in spite of the difference in mass fraction of functional fillers, the coatings exhibit basically the same characteristic peaks. Among them, 2960 cm^{-1} and 1453 cm^{-1} are respectively the absorption peaks of asymmetric stretching vibration, symmetrical stretching vibration, and asymmetric edges of methyl (CH_3) in acrylic resin; 1731 cm^{-1} is the absorption peak of stretching vibration of carbonyl (C=O) in acrylic resin; 770 $cm^{-1}$and 705 cm^{-1} are the absorption peaks of variable angular vibration of COO^- in acrylic resin; 3300 cm^{-1} is the absorption peak of stretching vibration of –NH of secondary amide in alkyl ammonium salt dispersant; 2854 $cm^{-1}$and 2925 cm^{-1} are the absorption peaks of symmetrical stretching and a symmetrical stretching of CH_2; 1636cm^{-1} is the absorption peak of stretching vibration of C=O in secondary amide; 1095 cm^{-1} is the absorption peak of the asymmetric stretching vibration of Si-O-Si; 847 cm^{-1} is the absorption peak of bending vibration of Si-OH; 470 cm^{-1} is the absorption peak of bending vibration of Si-O-Si. The last three absorption peaks are the characteristic absorption peaks of SiO_2 aerogel.

3.2.3 XRD analysis

Figure 4 displays the XRD images of SiO_2 aerogel composite insulation coatings of different formulas. As show in the figure, the coatings contain basically the same substances. The wide dispersion peak near 22° belongs to SiO_2 aerogel, the peaks near 27°, 36°, 42° and 54° probably belongs to titanium dioxide, the sharp peak near 22° may belong to hollow glass beads, and the peaks near 29° and 56° may come from the far-infrared ceramic powder. All of these peaks come from the raw materials of the coatings.

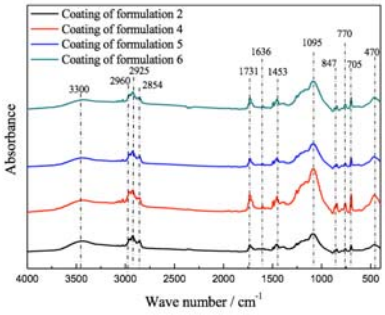

Figure 3: FT-IR images of SiO_2 aerogel composite thermal insulation coatings of different formulas

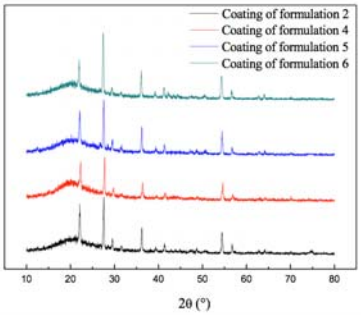

Figure 4: XRD images of SiO_2 aerogel composite thermal insulation coatings of different formulas

3.3. High temperature performance analysis of SiO2 aerogel composite thermal insulation coatings

3.3.1 XRD analysis

Figure 5 displays the XRD images of SiO_2 aerogel composite insulation coatings after being burned at different temperatures. As show in the figure, the characteristic peaks of the coatings of different formulas largely remains at the original location after being burned at 200°C, indicating that the coatings do not undergo chemical changes and products no new substance at the temperature. This means all of the coatings can withstand the temperature of 200°C. After being burned at 300°C, the coating of formula 2 exhibits characteristic peaks near 43°, 70° and 75°. In contrast, the same does not happen to the coatings of formulas

4, 5 & 6 for which the same peaks appear only after the coatings are burned at 400°. The reason is that cracks appear in the coatings as the temperature rises so that the characteristic peaks of low-carbon steel substrate materials appear in XRD images. Plus, as the mass fraction of SiO_2 aerogel in the coatings of formulas 4, 5 & 6 is higher than the coating of formula 2, indicating that the SiO_2 aerogel is conducive to the heat resistance of coating. What is more, the wide dispersion peak near 22° disappears after the coatings are burned at 400°C. This is probably caused by the formation of SiO_2 crystals after the coatings are burned at 400°C.

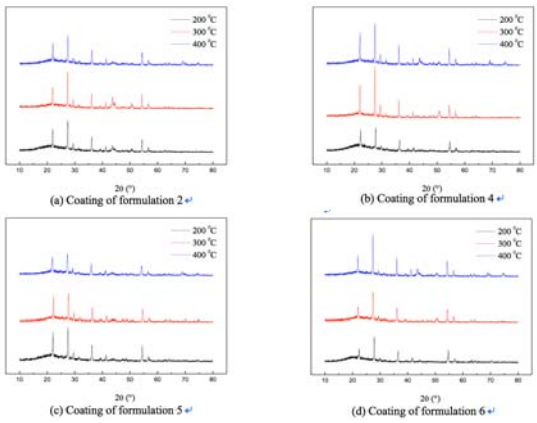

Figure 5: XRD images of the optimized coatings burn at different temperatures

3.3.2 FT-IR analysis

Figure 6 displays the FT-IR of SiO_2 aerogel composite insulation coatings of different formulas after being burned at different temperatures. In comparison with Figure 3, the characteristic peaks are not changed significantly after the coatings are burned at 200°C, but the intensity of some peaks are enhanced as the temperature rises. In light of the analysis of Figure 5, the intensity of the characteristic peak of Si-O-Si is greatly enhanced due to the formation of crystals, which is demonstrated by the sharp peaks at 1095 $cm^{-1}$and 470 cm^{-1}. Besides, through analysis of the images, the organics are not greatly affected by the firing at 200°C. However, when the temperature rises to 300°C, the characteristic peaks of organics in all coatings are reduced, indicating that some of the organics in the coatings are decomposed. When the temperature rises to 400°C, the characteristic peaks of organics almost disappear while those of inorganic substances become sharp and prominent.

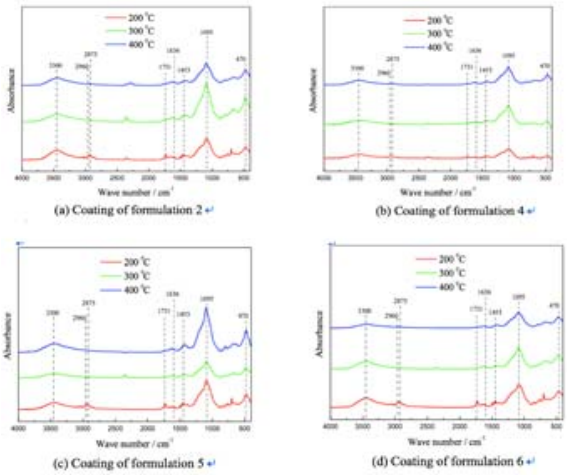

Figure 6: FT-IR images of the optimized coatings burn at different temperatures

4. Conclusion

1) Through the orthogonal experiment, the SiO_2 aerogel composite thermal insulation coating has the best performance when 5ωt% SiO_2 aerogel, 5ωt% titanium dioxide, 5ωt% hollow glass beads, and 10ωt% far-infrared ceramic powder are added. Besides, the thermal insulation performance of the coating gradually improves with the increase in wet film of the coating.

2) The hollow glass beads of the coatings form a continuous solar barrier layer and reflective layer, and SiO_2 aerogel, titanium dioxide and far-infrared ceramic powder further enhance the barrier efficiency of the coating and act as a reflector and radiator of sunlight, thereby greatly improving the thermal insulation performance of the coatings

3) The thermal insulation and high temperature performance of the thermal insulation coating increase with the mass fraction of the SiO_2 aerogel. When the SiO_2 aerogel is 5ωt%, the coating can withstand the temperature as high as 300°C.

Reference

Ameen K.B., Rajasekar K., Rajasekharan T., 2008, The effect of heat-treatment on the physico-chemical properties of silica aerogel prepared by sub-critical drying technique. Journal of Sol-Gel Science and Technology, 45(1), 9-15.

Boulaoued I., Amara I., Mhimid A., 2016, Experimental Determination of Thermal Conductivity and Diffusivity of New Building Insulating Materials, International Journal of Heat and Technology, 34(2), 325-331. DOI: 10.18280/ijht.340224.

Buratti C., Moretti E., Belloni E., 2016, Aerogel Plasters for Building Energy Efficiency. Nano and Biotech Based Materials for Energy Building Efficiency. Springer International Publishing, 17-40.

Cheng Y., Cheng S.L., 2012, Application and Discussion of Aerogels as Insulation Materials in Building Energy-saving. Building Energy Efficiency, 1, 019.

De Angelis A., Ceccotti L., Saro O., 2016, Cooling Energy Savings with Dry Cooler Equipped Plants in Office Buildings, International Journal of Heat and Technology, 34(S2), S205-S211. DOI: 10.18280/ijht.34S203.

Feng J., Mo W., Ma S., 2017, Thermal shrinkage inhibition mechanism of fumed silica based thermal insulating composite. Applied Thermal Engineering, 113, 749-755.

Garbarino J.M., Lion R.N., Saichi M., 2013, Spindle motor having connecting mechanism connecting lead wire and circuit board, and storage disk drive having the same: U.S. Patent Application 13/651,286[P].

Lang S., 2002, Current Situation and Progress of Energy Efficiency Design Standards in Buildings in China. Construction Machinery For Hydraulic Engineering & Power Station, 3.

Liang J.Z., 2014, Estimation of thermal conductivity for polypropylene/hollow glass bead composites. Composites Part B: Engineering, 56, 431-434.

Liu H., Chen J., 2005, Mechanism of thermal insulation coatings and its development. Materials review, 4(4).

Luca A.T., Paolo C., Claudia F., Federico S., 2016, Dynamic Behaviour and Control Strategy Optimization for Conventional Heating Plants in Buildings, International Journal of Heat and Technology, 34(S2), S505-S511. DOI: 10.18280/ijht.34S244.

Mario C., Vittorio F., Dimitrios K., Valerio M., 2013, Mario Cucumo, Vittorio Ferraro, Dimitrios Kaliakatsos, Valerio Marinelli, International Journal of Heat and Technology, 31(2), 111-118. DOI: 10.18280/ijht.310215.

Pierre A.C., Pajonk G.M., 2002, Chemistry of aerogels and their applications. Chemical Reviews, 102(11), 4243-4266.

Qu J., Song J., Qin J., 2014, Transparent thermal insulation coatings for energy efficient glass windows and curtain walls. Energy and Buildings, 77, 1-10.

Roselli C., Sasso M., Tariello F., 2016, Dynamic Simulation of a Solar Electric Driven Heat Pump Integrated with Electric Storage for an Office Building Located in Southern Italy, International Journal of Heat and Technology, 34(4), 637-646. DOI: 10.18280/ijht.340413.

Wei T.Y., Lu S.Y., Chang Y.C., 2008, Transparent, hydrophobic composite aerogels with high mechanical strength and low high-temperature thermal conductivities. The Journal of Physical Chemistry B, 112(38), 11881-11886.

Woignier T., Phalippou J., Vacher R., 1990, Different kinds of fractal structures in silica aerogels. Journal of Non-Crystalline Solids, 121(1), 198-201.

Xia Z., Tu W., Yang Z., 2001, Advances in development of thermal insulation coatings. FINE CHEMICALS-DALIAN-, 18(10), 599-602.

Zhao J., Du F., Cui W., 2014, Effect of silica coating thickness on the thermal conductivity of polyurethane/SiO 2 coated multiwalled carbon nanotube composites. Composites Part A: Applied Science and Manufacturing, 58, 1-6.

Zhou B., Chen Z.Q., 2016, Experimental Study on the Hygrothermal Performance of Zeolite-Based Humidity Control Building Materials, International Journal of Heat and Technology, 34(3), 407-414. DOI: 10.18280/ijht.340309.